SUPPLEMENTARY MATERIAL

METHODS

Magnetic resonance imaging protocol

Magnetic resonance imaging (MRI) was performed for all subjects at 3T (MAGNETOM Trio Siemens, Erlangen, Germany). The protocol included a 3D T1-weighted magnetization prepared rapid acquisition gradient echo (MPRAGE) sequence (repetition time (TR) =1900 ms, echo time (TE) =3.03 ms, isotropic resolution 1x1x1 mm), and a 3D T2-weighted fluid-attenuated inversion recovery (FLAIR) sequence (TR = 6000 ms, TE = 388 ms, isotropic resolution 1x1x1 mm) of the brain.

Measurement of thalamic volume and thalamic nuclei volume using the MAGeT brain algorithm

The Multiple Automatically Generated Templates (MAGeT) brain algorithm [1,2] was used to segment the entire thalami and the different thalamic nuclei on MPRAGE MR images. MAGeT uses an atlas derived from manually segmented serial histological data, containing delineation of the thalamic nuclei, as per Hirai and Jones [3]. It first customizes the atlas to a subset of participants, representative of the entire study population, using a nonlinear registration scheme.

In our study, this representative subset was chosen in a manner consistent with best practices for the algorithm [4], according to age, sex and - for patients - number and type of attacks. It consisted of eleven NMOSD patients (ten women, mean age: 50±15.1 years, median number of attacks 3 (range 1-11), 10/11 with myelitis and 7/11 with ON) and ten controls (9 women, mean age: 47.4±12 years). This newly segmented subset acted as a template library for the remaining participants, to correct for the neuroanatomical variability of our study population and to average different sources of random error prior to the final segmentation [5].

Lesions in the thalamus and the optic radiations

The 3D T2-weighted fluid-attenuated inversion recovery (FLAIR) images of patients were assessed and verified for thalamic- and optic radiations (OR) lesions in consensus by a board-certified neurologist (A.P.) and a board-certified radiologist (M.S.), to assess whether lesions in these strategic locations may influence our results.

Mean upper cervical cord area

The mean upper cervical cord area (MUCCA) was used as a sensitive measure to assess spinal cord atrophy in patients with NMOSD [6]. MUCCA was measured in 3D MPRAGE images using an active surface model [7] by averaging the cross-sectional areas from five consecutive slices at the C2/C3 intervertebral space level, as described previously [6,8].

Optical coherence tomography: excluded scans and scanning protocol

Retinal imaging was performed using a Heidelberg Engineering Spectralis spectral domain optical coherence tomography (OCT; Heidelberg Engineering, Heidelberg, Germany), with ART (automatic real-time) function for image averaging. We did not use pupil dilation. All patients had the OCT on the same day as the MRI and clinical examination, except for two, where there was an interval of one day. For the controls there was often an interval of few days between OCT and MRI/clinical assessment (on average: 7.4±11.7 days, range 0-50 days).

A total of ten eyes from eight patients had to be excluded from the analysis: six eyes due to incidental findings, three due to lack of OCT data, and one due to quality reasons, according to the OSCAR-IB criteria. For two additional eyes, only the macular scan had to be excluded, due to quality reasons [9].

The OCT acquisition settings and scanning protocol are reported below, according to the APOSTEL recommendations [10]:

The peripapillary retinal nerve fiber layer (pRNFL) was measured using 3.4-mm ring scans around the optic nerve head (12°, 1536 A-scans, 9≤ ART ≤100). The combined ganglion cell and inner plexiform layer (GCIPL) volume was measured using a 6-mm diameter cylinder around the fovea from a macular volume scan (25°x30°, 61 vertical B-scans, 768 A-scans per B-scan, ART=15). Segmentation of the pRNFL and the intraretinal layers in the macular scan was performed semi-automatically using software provided by the optical coherence tomography manufacturer (Eye Explorer 1.9.10.0 with viewing module 6.0.9.0; Heidelberg Engineering). All measurements were checked for segmentation errors and corrected if necessary, by one experienced rater (F.C.O.).

RESULTS

Volume of the LGN: differences between ipsilateral and contralateral side to optic neuritis (ON)

Since the LGN of both hemispheres receive afferences from each optic nerve, both LGN were expected to be affected similarly after a unilateral ON episode.

To confirm this, we performed an additional analysis comparing the LGN volume between patients with ON (NMO-ON) and without ON (NMO-NON) separately for unilateral LGN to ON and contralateral LGN to ON. From this analysis, 12 NMO-ON patients with bilateral ON were excluded. From the included NMO-ON patients (n=13), 6 patients had ON on the left eye and 7 patients on the right eye. The NMO-NON patients were 14.

This analysis was performed using linear mixed effect models (LMM), with LGN volume being the dependent variable, ON history fixed effect, next to age and sex, and subject and side random effects.

Although the volume of ipsilateral to ON LGN was smaller than the LGN volume of NMO-NON patients (B=-21.10, SE= 8.69, p= 0.023, mR2= 0.05, cR2= 0.94), this was not the case for contralateral LGN to ON (B= -16.29, SE= 7.99, p= 0.052, mR2= 0.02, cR2=0.95). However, the latter was a borderline not significant result, the p value being 0.052, and could be also due to the lower power of this subgroup analysis, which included a total of 41 LGN.

REFERENCES

1 Chakravarty MM, Bertrand G, Hodge CP, *et al.* The creation of a brain atlas for image guided neurosurgery using serial histological data. *NeuroImage* 2006;**30**:359–76. doi:10.1016/j.neuroimage.2005.09.041

2 Chakravarty MM, Steadman P, van Eede MC, *et al.* Performing label-fusion-based segmentation using multiple automatically generated templates. *Hum Brain Mapp* 2013;**34**:2635–54. doi:10.1002/hbm.22092

3 Hirai T, Jones EG. A new parcellation of the human thalamus on the basis of histochemical staining. *Brain Res Brain Res Rev* 1989;**14**:1–34.

4 Pipitone J, Park MTM, Winterburn J, *et al.* Multi-atlas segmentation of the whole hippocampus and subfields using multiple automatically generated templates. *NeuroImage* 2014;**101**:494–512. doi:10.1016/j.neuroimage.2014.04.054

5 Magon S, Chakravarty MM, Amann M, *et al.* Label-fusion-segmentation and deformation-based shape analysis of deep gray matter in multiple sclerosis: the impact of thalamic subnuclei on disability. *Hum Brain Mapp* 2014;**35**:4193–203. doi:10.1002/hbm.22470

6 Chien C, Scheel M, Schmitz-Hübsch T, *et al.* Spinal cord lesions and atrophy in NMOSD with AQP4-IgG and MOG-IgG associated autoimmunity. *Mult Scler Houndmills Basingstoke Engl* 2018;:1352458518815596. doi:10.1177/1352458518815596

7 Horsfield MA, Sala S, Neema M, *et al.* Rapid semi-automatic segmentation of the spinal cord from magnetic resonance images: application in multiple sclerosis. *NeuroImage* 2010;**50**:446–55. doi:10.1016/j.neuroimage.2009.12.121

8 Losseff NA, Webb SL, O'Riordan JI, *et al.* Spinal cord atrophy and disability in multiple sclerosis. A new reproducible and sensitive MRI method with potential to monitor disease progression. *Brain J Neurol* 1996;**119 (Pt 3)**:701–8.

9 Tewarie P, Balk L, Costello F, *et al.* The OSCAR-IB consensus criteria for retinal OCT quality assessment. *PloS One* 2012;**7**:e34823. doi:10.1371/journal.pone.0034823

10 Cruz-Herranz A, Balk LJ, Oberwahrenbrock T, *et al.* The APOSTEL recommendations for reporting quantitative optical coherence tomography studies. *Neurology* 2016;**86**:2303–9. doi:10.1212/WNL.0000000000002774

SUPPLEMENTARY FIGURES

Supplementary Figure 1: LGN segmentation by MAGeT

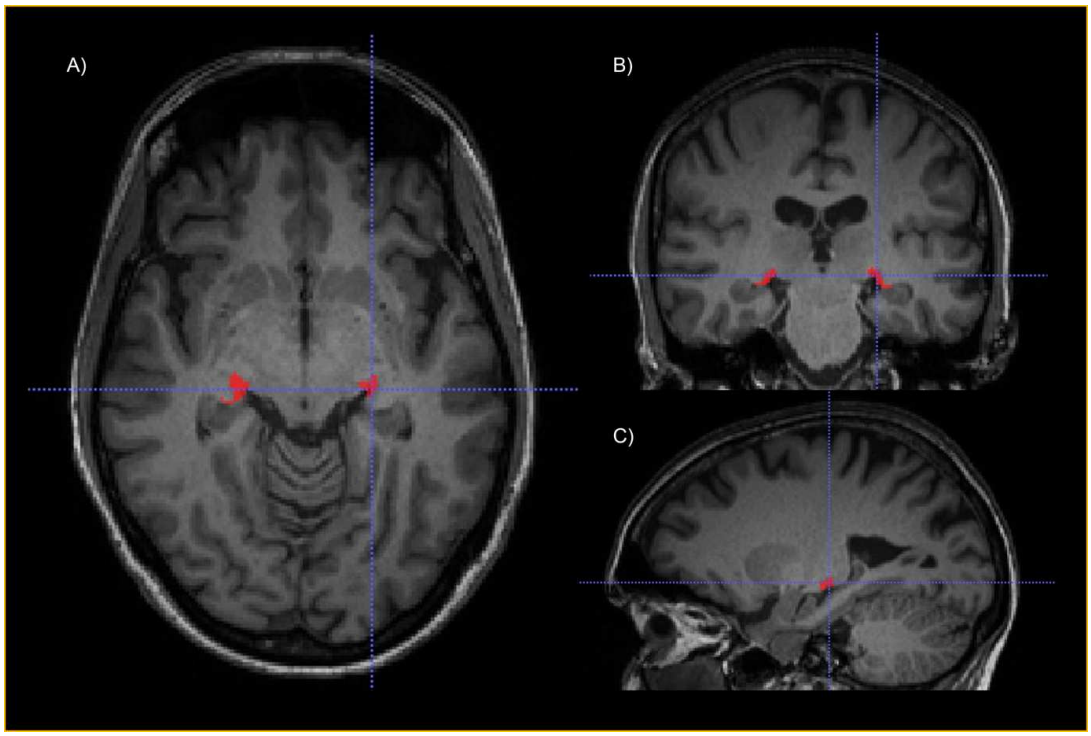

Legend: The figure shows an example of the lateral geniculate nucleus (LGN) segmentation in a control subject, as performed by the MAGeT brain algorithm[1,2]. The LGN is shown in red at: A) axial, B) coronal and C) sagittal view, on a 3D T1-weighted magnetization prepared rapid acquisition gradient echo (MPRAGE) sequence.

Supplementary Figure 2: VPN Segmentation by MAGeT

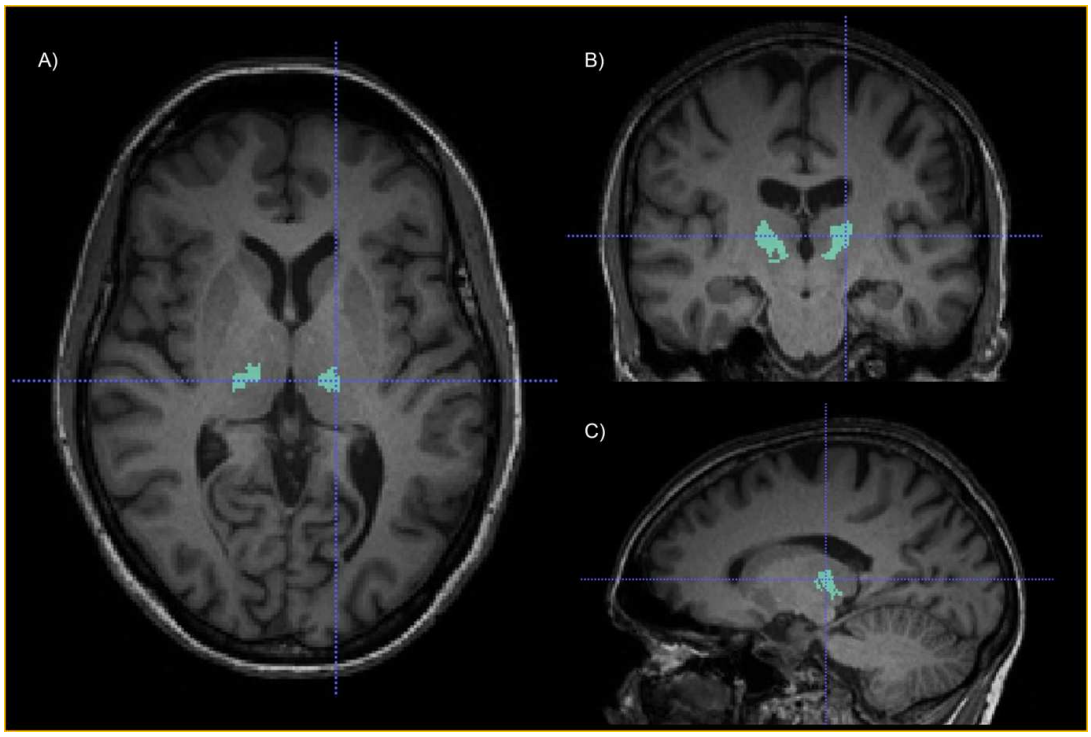

Legend: The figure shows an example of the ventral posterior nucleus (VPN) segmentation in a control subject, as performed by the MAGeT brain algorithm[1,2]. The VPN is shown in turquoise at: A) axial, B) coronal and C) sagittal view, on a 3D T1-weighted magnetization prepared rapid acquisition gradient echo (MPRAGE) sequence.